

# The modal analysis of laminated composite cylinders under axial tension loading in ANSYS

*Andrejs Kovalovs*<sup>1\*</sup>, *Andris Chate*<sup>1</sup> and *Vladimir Kulakov*<sup>2</sup>

<sup>1</sup>Institute of Materials and Structures, Riga Technical University, Kipsalas Street, 6A, LV-1048 Riga, Latvia

<sup>2</sup>Institute of Mechanics for Materials, University of Latvia, Aizkraukles Street, 23, LV-1006, Riga, Latvia

**Abstract.** Natural frequencies and vibration modes of laminated composite cylinders were calculated under axial tension loading by the finite element method using ANSYS Mechanical software package. Two types of axial tensile load were modelled: a suspended weight and a static axial load in the zone of weight attachment into the cylinder. The features of the modal analysis of a prestressed system depending on the type of applied tensile load were analyzed. The numerical results obtained were compared and the possible reasons for their discrepancy were explained.

## 1 Introduction

Cylindrical multi-layered composite shells are one of the most common structural members used in mechanical, marine, aerospace, and civil engineering structures. This is due to their relatively low density and good strength characteristics. However, technical state of a structure changes in the process of its intensive operation, technological defects, and random mechanical actions, which leads to a decrease of its reliability and strength. Therefore, structural health monitoring is required in order to ensure strength, durability and estimation of the structure lifetime. At present, in the practice of non-destructive testing for the detection of defects, almost all methods and techniques traditionally applied in the conditions of production, testing and operation of the parts and unit assemblies are used. They include optical, electrical, acoustic, radiation, magnetic, thermal, holographic, microwave, and other control methods [1, 2].

Vibration testing is one of the effective types of non-destructive testing which is based on monitoring and analysis of key indicators of vibrations measured during the object investigation. The structure in this case can be excited by the loudspeaker, PZT and MFC actuators, PCB impulse hammer or shaker depending on the investigated object's dimensions, weight and dissipative properties [3, 4, 5]. The dynamic response is measured in most cases by accelerometers or by non-contact optical sensing using scanning laser vibrometers [3]. To obtain modal parameters, such as vibration modes, natural frequencies, and damping factors, free vibration [6], frequency [7] and transient [8] response analyses are applied. These dynamic parameters are used as a so-called passport for estimation structural

---

\* Corresponding author: [andrejs.kovalovs@rtu.lv](mailto:andrejs.kovalovs@rtu.lv)

health monitoring of the structure during its operation. The deviation of the current modal parameters from the initial ones indicates the origination of damage [9, 10]. To date, many classical [11, 12] and modern works have been devoted to the study of shell vibrations [13, 14].

Static loads acting on the cylindrical structures during their operation lead to a change of their geometry and modal parameters. The study of prestressed and unstressed systems revealed the difference of their mechanical characteristics (natural frequencies and vibration modes) [15]. The influence of internal stresses from an axial load on the dynamic response was considered in the classic work of Leis and Coedel [16, 17], where the expression for the natural frequency of a cylindrical shell, depending on the action of a tensile or compressive force, was obtained. An increase of tensile axial force on a cylindrical shell increases its natural vibration frequencies, whereas the action of a compressive axial force leads to a decrease of the natural frequencies. An analysis of scientific literature has shown that many works were devoted to the vibrations of cylindrical shells under the action of a compressive axial force, which include experimental research, analytical and numerical calculations [18, 19].

Much less attention has been paid to the study of an influence of a tensile axial force on the natural frequencies and vibration modes of cylindrical composite shells. With respect of the numerical calculation of the cylindrical composite shells by numerical methods, we can note the works of Tong [20] and Bedri [21]. Tong L., using the classical theory of shells, calculated the natural frequencies of conical shells with different geometry and boundary conditions under the action of axial loads. The results showed that axial tension of the conical shells increases their natural frequencies, while axial compression reduces. Using the ANSYS finite element program, Bedri performed a modal analysis of a metal cylindrical cone under the action of a tensile or compressive axial force. The numerical results confirmed the dependence of the values of natural frequencies on action of a tensile or compressive force. The natural frequencies of a cylindrical shell decrease in the case of compressive force and increase in the case of tensile force action.

The current work was carried out as a part of the project devoted to the development of a prototype for a monitoring system of the existing structure. Laminated composite cylinders are the objects of the study. One of the sections of the project investigates the experimental effect of axial tensile force on the dynamic characteristics of a composite shell with an embedded sensor system using Operational Modal Analysis methods. The objective of this work is a preliminary study of the effect of axial tensile load on natural frequencies and vibration modes of a composite cylindrical shell structure according to the planned experiment.

## 2 Materials and methods

### 2.1 Solution methodology

The finite element method (FEM) was used to estimate the effect of static load on the modal properties of the composite shell structure [22]. If damping is neglected, the natural vibrations of the finite element (FE) model are described in matrix form by the equation:

$$[K]\{u\} + [M]\{\ddot{u}\} = \{0\}, \quad (1)$$

Where  $[K]$  and  $[M]$  are the stiffness and mass matrices, respectively,  $\{u\}$  and  $\{\ddot{u}\}$  are the vectors of displacements and accelerations  $e$  in the nodes of FE model, respectively.

This equation has a real periodic solution of the form  $\{u\} = \{\varphi\} \cos \omega t$  if the following condition is

$$([K] - \omega_i^2 [M])\{\varphi\}_i = \{0\}, \tag{2}$$

Where  $\{\varphi\}$  is the eigenvector,  $\omega$  is the natural frequency,  $t$  is the time.

For modal analysis with prestressing, the static loading problem of the structure is solved firstly. Then, the modal analysis is performed using the stresses determined as a result of a constant load, which can affect the natural frequency of the structure. For static analysis, the following equation is used:

$$[K]\{x\} = \{F\}, \tag{3}$$

where  $\{F\}$  is the force vector,  $\{x\}$  is the displacement vector. As a result of structural static analysis, a stress stiffness matrix  $[K]_g$  is determined, which is added to the regular stiffness matrix  $[K]$  performing modal analysis of prestressed structure. Thus, the modal analysis of the structure, taking into account prestressing, is performed based on the following equation:

$$([K]_{total} - \omega_i^2 [M])\{\varphi\}_i = \{0\}, \tag{4}$$

where  $[K]_{total} = [K] + [K]_g$ .

## 2.2 Laminated Composite Cylinders

The composite cylindrical structure investigated consists of a central part, which is a multi-layered composite cylinder composed from four layers of a cross-ply fiberglass fabric. The layers of fiberglass fabric are placed in such a way that the reinforcing fibers are oriented at an angle of 45° to the axis of the cylinder. Plywood flanges are glued to the end surfaces of the cylinder, which increase the mechanical rigidity of the structure (Fig. 1a). Thickness of plywood flanges is 31 mm. The inner and outer diameters are 240 and 360 mm, respectively.

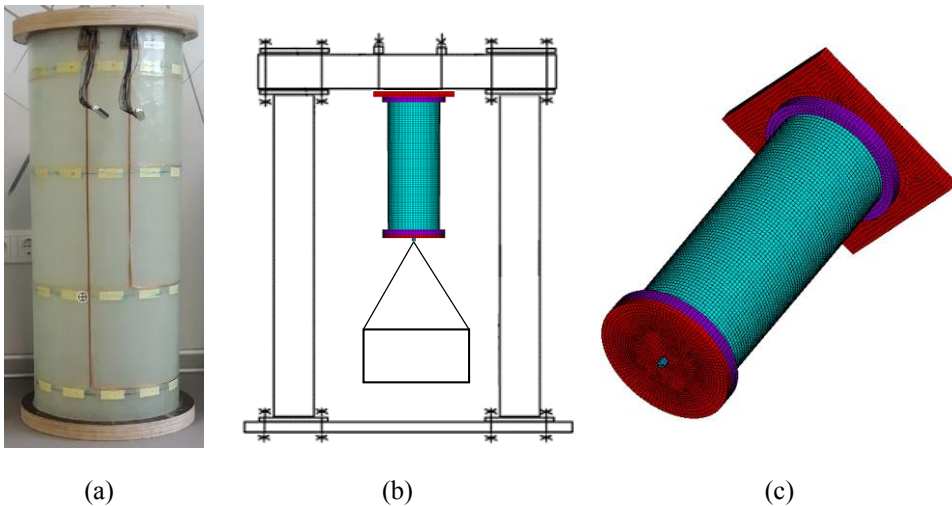


**Fig. 1.** (a) Composite structure; (b) Test bench; (c) FE model.

The total height of the cylinder is 790 mm. The wall thickness of composite cylinder is  $1.45 \pm 0.05$  mm. The total mass of each composite structure (composite cylinder, wires, and plywood flanges) was  $4.58 \pm 0.1$  kg.

The composite structure testing under static load is planned on a test bench (Fig. 1b). The composite structure is mounted vertically on the test stand and fixed by means the top flange to the top plywood board attached to the top beam of the stand. The static load test is carried out by hanging a basket with a weight to the bottom flange.

To do this, a round plywood cover is fixed to the flange with a ring lug for attaching the basket ropes. The thickness of the plywood cover is 18 mm. The total weight of the bottom plywood cover with ring lug is 2.3 kg.

The problem of the effect of axial tensile load on natural frequencies and vibration modes was solved by the finite element method using the ANSYS Mechanical software package. To model a layered composite shell, a Shell181 four-node finite element with six degrees of freedom at the nodes was used. The plywood flanges, cover plate, and basket with a weight were modelled using a 3D 8-node SOLID185 element (Fig. 1c). For modelling the basket ropes, a 3D linear beam element BEAM 188 accounting for the finite strains was chosen.

The load on the composite cylinder is varied from 167 N to 4817 N. The initial load of 167 N includes the weight of the plywood cover plate with ring lug and the weight of the basket (Fig. 2a). The load step of 665 N was chosen taking into account the mass of concrete blocks that will be loaded into the basket. The calculation was carried out taking into account the own weight of the structure. The gravitational acceleration of  $9.81 \text{ m/s}^2$  is included in the calculation to account for the mass of the composite structure with the plywood cover plate, as well as to simulate the axial tensile force arising from the weight of the loaded basket. The distance between the bottom cover and the weight is 1 m. The diameter of ropes is 10 mm. The basket with the weight was modelled as a rectangular parallelepiped of  $340 \times 500 \times 840$  mm in size. The suspended weight was controlled by changing the density of the parallelepiped material. The mass of ropes was also taken into account.

The next stage of the calculation was the modelling of a composite cylindrical structure without basket. An axial tensile force corresponding to the mass of the basket with the weight was applied through the ring lug (Fig. 2b). In addition, the influence of the axial tensile load on the natural frequencies of the cylinder without weight was studied, when the tensile force was applied in the zone of the ends of the cylinder, which corresponds to pure tension (Fig. 2c).

The mechanical properties of plywood, steel, and fiber rope are presented in Table 1.

**Table 1.** Mechanical properties of materials.

Elastic constants	Plywood [23]	Steel	Fiber rope [24]
$E_l$ , GPa	17.0	210	130
$\nu$	0.3	0.3	0.3
$\rho$ , $\text{kg/m}^3$	685	7850	2000

It should be noted that, taking into account the manufacturing technology of the composite structure, the density of plywood flanges is assumed to be  $\rho = 810 \text{ kg/m}^3$ , which differs from the nominal value ( $685 \text{ kg/m}^3$ ). This is due to the peculiarities of gluing the composite cylinder and flanges. The steel ring lug was modelled in the form of a rod, to which the ropes were attached. The dimensions of the metal rod were chosen so that, taking into account the density of plywood and metal, the total mass of the model of the bottom plywood plate and the ring lug was 2.3 kg. Dyneema fiber ropes are made from Ultra-High Molecular Weight Polyethylene.

The density of the composite material is assumed to be  $\rho = 1850 \text{ kg/m}^3$ . The total mass of the FEM model was 4.58 kg, which corresponds to the weight of a real composite structure consisting of a composite shell and plywood flanges. The mechanical properties of fiberglass were determined by calibrating the finite element model by the method of identification of the elasticity characteristics of the material. The size of the finite element of the FEM model was chosen by means of a series of calculations and evaluation of the convergence of the solution. According to the results of convergence, the size of the finite element is  $10 \times 10$  mm [25].

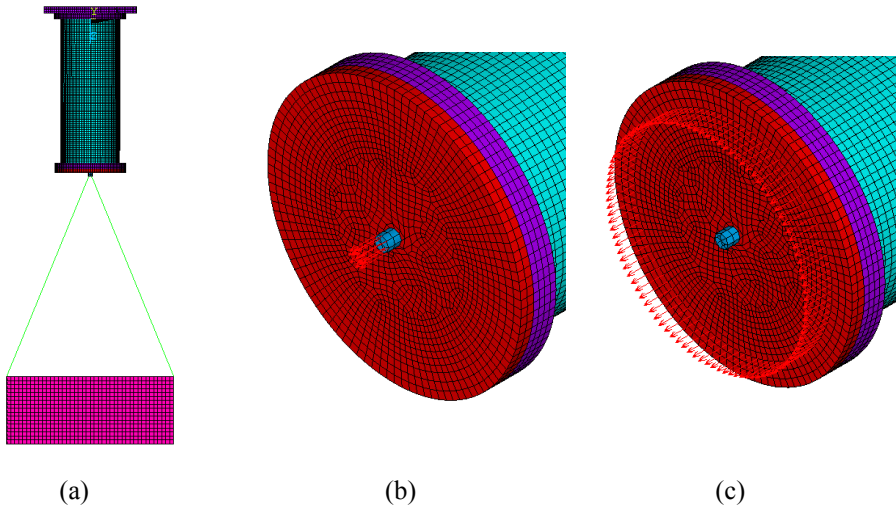


**Fig. 2.** Modelling of axial tensile force: (a) basket with the weight; (b) axial tensile force applied through the ring lug; (c) axial tensile force applied to the ends of the cylinder.

### 2.3 Calibration of Finite Element Model

To refine the elastic properties of the composite monolayer, the finite element model was calibrated. The properties of the composite material were determined using an identification method based on solving the inverse problem [26, 27] and including several stages based on [28].

At the first stage, to determine the natural frequencies and vibration modes, we performed an experimental modal analysis of a composite structure consisting of a layered shell and two plywood flanges. The experimental values of natural frequencies and vibration modes are taken from [29]. The dynamic characteristics of the specimen 3 were chosen for further calibration of the FEM model. At the next stage, we developed an experiment plan for all characteristics of the composite material (Young's moduli:  $E_1, E_2 = E_3$ , shear moduli:  $G_{12} = G_{13}, G_{23}$ , Poisson's ratios:  $\nu_{12} = \nu_{13}, \nu_{23}$ ) with a deviation from some a priori values of the material taken on based on the data published in literature and estimates [30]. Then, a FEM model was developed and, according to the experimental plan developed, a numerical calculation was carried out. Based on the results of numerical simulation, approximation functions were constructed for each frequency. The main stage of the identification procedure of material properties is the usage of the approximation functions obtained and experimental data. The solution of the problem of identification of a composite material was considered as an optimization problem [31] with the objective function:

$$\Phi_i(\mathbf{x}) = \sum_{i=1}^m \frac{(f_i^{\text{exp}} - f_i^{\text{FEM}})^2}{(f_i^{\text{exp}})^2} \Rightarrow \min. \quad (5)$$

where  $f_i^{\text{FEM}}$  and  $f_i^{\text{exp}}$  are the calculated and experimental values of the first natural frequency, respectively.

The elastic characteristics determined are presented in Table 2.

**Table 2.** The identified engineering constants.

Engineering constants	$E_1$ , GPa	$E_2 = E_3$ , GPa	$G_{12} = G_{13}$ , GPa	$G_{23}$ , GPa	$\nu_{12} = \nu_{13}$	$\nu_{23}$
Value	41.39	11.75	1.75	2.86	0.407	0.35

To estimate the accuracy of the composite structure model developed, the first 14 natural frequencies and vibration modes were calculated with the elastic characteristics of the composite material identified. A comparison of the calculated values of natural frequencies with the experimental ones is presented in Table 3. For structures with axial symmetry, the presence of multiple natural frequencies is characteristic, therefore, the calculated values of natural frequencies have paired values. The discrepancy between the calculated and experimental data is mainly within 6%. The difference in the values of the natural frequencies for the mode (1,2) and the mode (1,1) drops out somewhat.

**Table 3.** Comparison of calculated and experimental values of natural frequencies of composite structure.

Order	Mode	Exp.	FEM	Error
	(m,n)	Hz	Hz	%
1.	(1,1)	78.8	92.8	–
2.	(1,1 <sup>a</sup> )	104.0	92.8	10.8
3.	(1,4)	179.5 <sup>b</sup>	178.4	0.6
4.	(1,4 <sup>a</sup> )	178.9 <sup>b</sup>	178.4	0.3
5.	(1,3)	183.3 <sup>b</sup>	194.8	6.3
6.	(1,3 <sup>a</sup> )	188.4 <sup>b</sup>	194.8	3.4
7.	(1,5)	238.7 <sup>b</sup>	234.9	1.6
8.	(1,5 <sup>a</sup> )	239.2 <sup>b</sup>	234.9	1.8
9.	(1,2)	257.0 <sup>b</sup>	304.9	18.6
10.	(1,2 <sup>a</sup> )	263.5 <sup>b</sup>	304.9	15.7
11.	(2,5)	324.2 <sup>b</sup>	317.4	2.1
12.	(2,5 <sup>a</sup> )	324.2 <sup>b</sup>	317.4	2.1
13.	(1,6)	333.7	329.5	1.3
14.	(1,6 <sup>a</sup> )	–	329.5	–

<sup>a</sup> Eigenmode with multiple frequency; <sup>b</sup> Frequencies involved in identification process.

### 3 Results and discussion

At the first stage, a static problem was solved for three types of loading of composite cylinders: with a weight in the basket, with a force applied through the ring lug, and a force applied to the bottom end of the cylinder. For all calculations, the similar graphical dependence of the structure displacement on the tensile force was obtained (Fig. 3). The displacement was captured at the bottom end of the composite cylinders. The resulting dependence shows the coincidence of the basket weight calculated and the force applied.

At the second stage, the problem of determining the natural vibration frequencies of a cylindrical composite structure was solved. Table 4 shows the calculation results of natural vibration frequencies for cylinders with a force applied through the ring lug and with a force applied to the bottom end of the cylinder. To determine the percentage difference of an influence of the tensile force on the natural frequencies of the cylinders, the results of calculating the natural frequencies of vibrations at the minimum and maximum values of the tensile force are given. The total values of pair frequencies for each mode are presented.

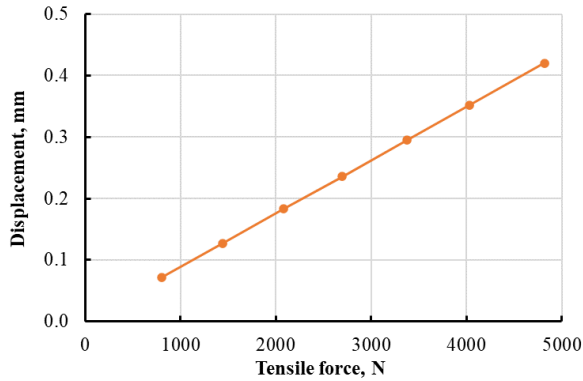


**Fig. 3.** Dependence of displacement vs. tensile force.

As follows from the data in Table 4, the calculations of natural vibration frequencies of cylinders with two types of tensile load application gave practically the same results and, accordingly, the same values of percentage change.

**Table 4.** Percentage change for cylinders with a force.

Order	Mode (m,n)	Force applied through the ring lug			Force applied to the bottom end of cylinder		
		Tensile force, N		Percentage change Δ, %	Tensile force, N		Percentage change Δ, %
		167, N	4817, N		167, N	4817, N	
1.	(1,1)	60.24	60.62	0.64	60.24	60.63	0.65
2.	(1,4)	179.51	182.66	1.75	179.51	182.62	1.73
3.	(1,3)	203.09	206.04	1.45	203.09	205.95	1.41
4.	(1,5)	235.11	237.55	1.04	235.11	237.54	1.03
5.	(1,0)	252.35	252.53	0.07	—	—	—
6.	(2,5)	318.35	324.89	2.05	318.35	324.81	2.03
7.	(1,6)	329.54	331.38	0.56	329.54	331.37	0.55
8.	(1,0)	—	—	—	252.35	252.55	0.08
9.	(1,2)	341.35	343.26	0.56	341.31	343.15	0.54
10.	(2,4)	350.25	356.36	1.75	350.25	356.24	1.71
11.	(2,6)	375.91	381.46	1.48	375.91	381.42	1.47

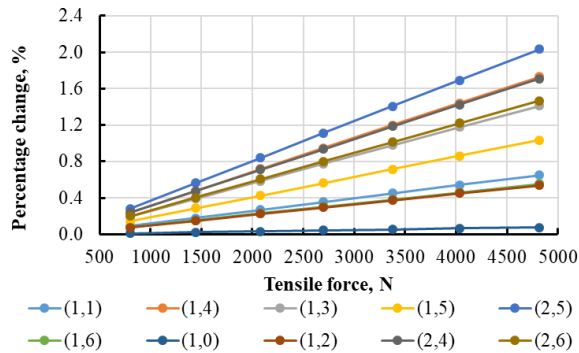


**Fig. 4.** Percentage change in the case of force applied through the ring lug.

The sequence of the main vibration modes is preserved. The exception is the vibration mode (1,0), which appears earlier in the model with a force applied through the ring lug. The maximum percentage difference of  $\sim 2.0\%$  corresponds to the vibration mode (2,5). The graphical dependence of percentage changes on the tensile force applied through the ring lug is shown in Fig. 4. The force of 167 N was chosen as a reference one. The results of the modal analysis in the form of vibration modes of the layered shell are presented in Fig. 5. The vibration modes are presented as diagrams of the structure displacements in the relative values.

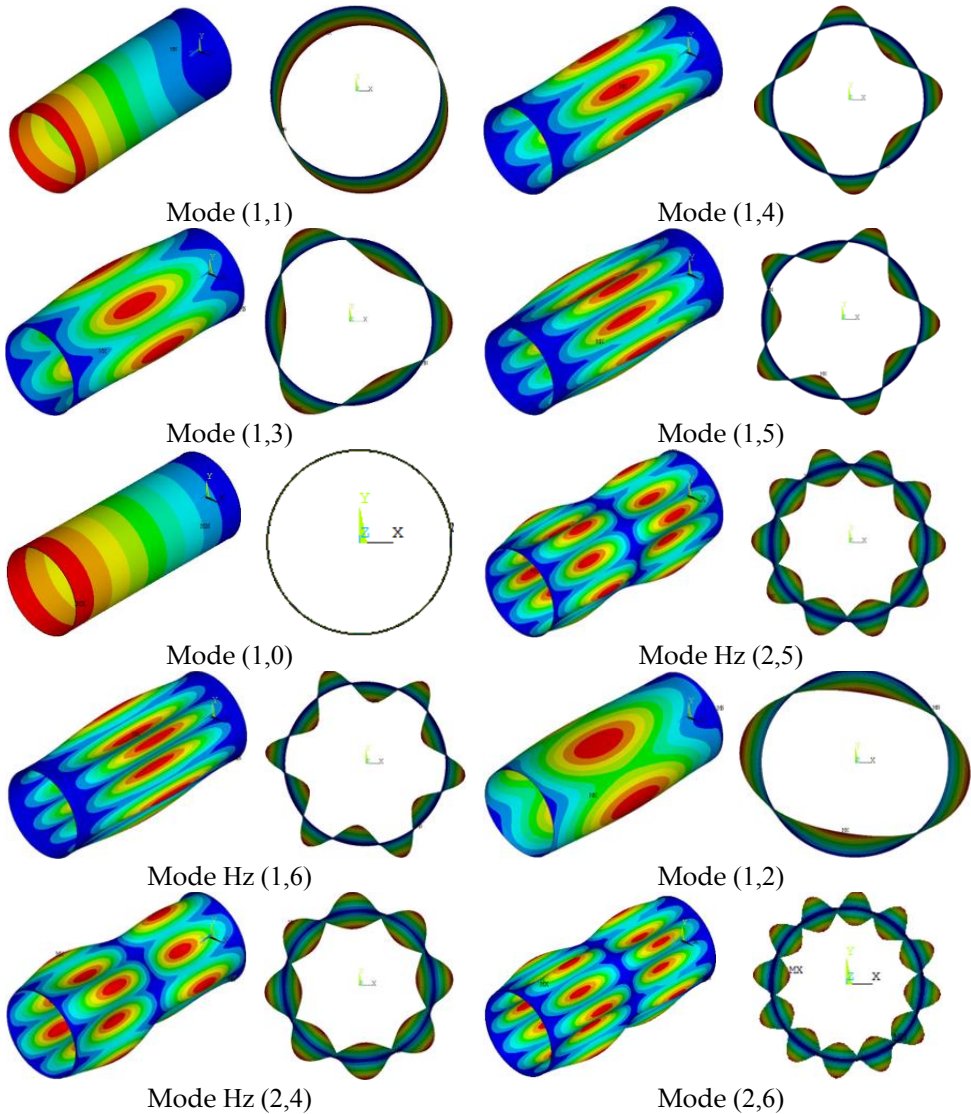


**Fig. 5.** Axial and circumferential eigenmodes.

Table 5 demonstrates the results of calculations of the minimum and maximum values of natural vibration frequencies of a cylinder with a suspended weight. The graphical dependence of the percentage changes in the range of applied tensile load is presented in Figures 6a and 6b.

**Table 5.** Percentage change for cylinder with a suspended weight.

Order	Mode (m,n)	Tensile force, N		Percentage change
		167, N	4817, N	$\Delta$ , %
1.	(1,1)	54.82	22.51	-58.94
2.	(1,1)	57.51	29.78	-48.21
3.	(1,0 <sup>a</sup> )	96.84	17.64	-81.78
4.	(1,1 <sup>a</sup> )	190.12	124.61	-34.46
5.	(1,4)	179.51	182.61	1.73
6.	(1,3)	203.09	205.95	1.41
7.	(1,1)	254.24	194.77	-23.39
8.	(1,5)	235.11	237.53	1.03
9.	(2,5)	318.35	324.81	2.03
10.	(1,6)	329.54	331.37	0.55
11.	(1,2)	341.31	343.15	0.54
12.	(2,4)	350.25	356.23	1.71
13.	(2,6)	375.91	381.42	1.47

<sup>a</sup> Eigenmode with multiple frequency that were defined since 1440 N.

During calculations, the ropes were modelled with one finite element in thickness, because the use of several elements increases the processing time of the results, demonstrating not only the vibration modes of the cylinder, but also the ropes (Fig. 7a). The change of the number of elements for modelling the ropes did not affect the vibration modes and values of natural frequencies of the cylinder.

As can be seen from the data in Table 5, there are several bending modes (1,1), the value of natural vibration frequencies of which decreases with increasing the tensile load. This trend is also observed for the tension mode (1,0). The largest percentage change of ~82% was observed for vibration mode (1,0). Percentage change for these modes is nonlinear (Fig. 6b).

Visual analysis of the tension (Fig. 7b) and bending (Fig. 7c) vibration modes shows the combined operation of the cylinder and the suspended weight. For all other modes, an increase of the values of natural vibration frequencies was observed depending on the increasing the weight of the basket (Fig. 6a).

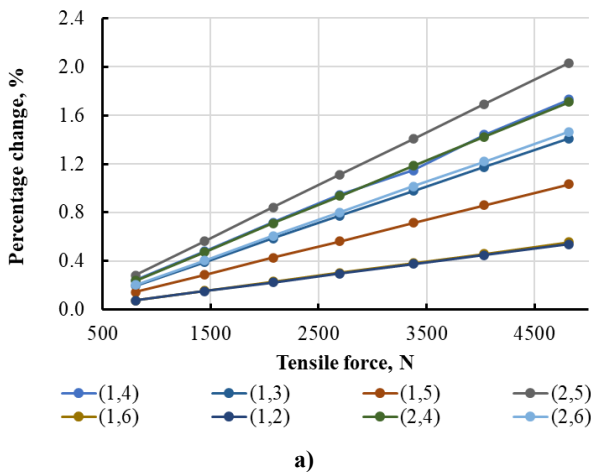


**Fig. 6.** Percentage change dependence on tensile force: (a) positive dependence.

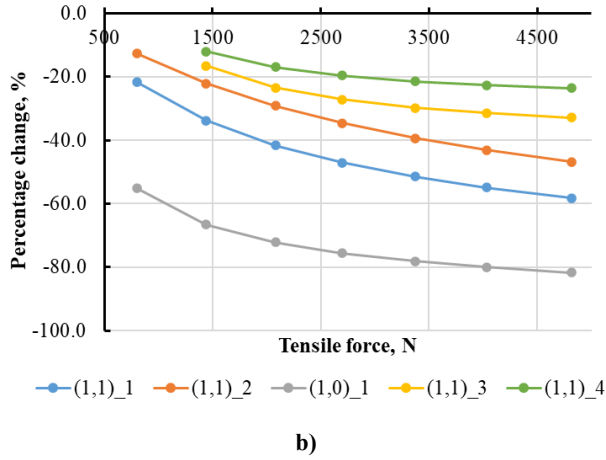


**Fig. 6 continued.** Percentage change dependence on tensile force: (b) negative dependence.

Vibration modes only were originated in the composite cylinder (Fig. 7d and 7e). The values of natural vibration frequencies coincide with the results of the modal analysis of the cylindrical composite structure with a force applied through the ring lug.

One of the possible explanations of the decreasing the natural frequencies of the vibration modes (1,1) and (1,0) is the coupled vibrations of the system, which includes the vibration modes of the cylinder and suspended weight. Accordingly, the values of natural vibrations frequencies decrease with an increasing the system mass.

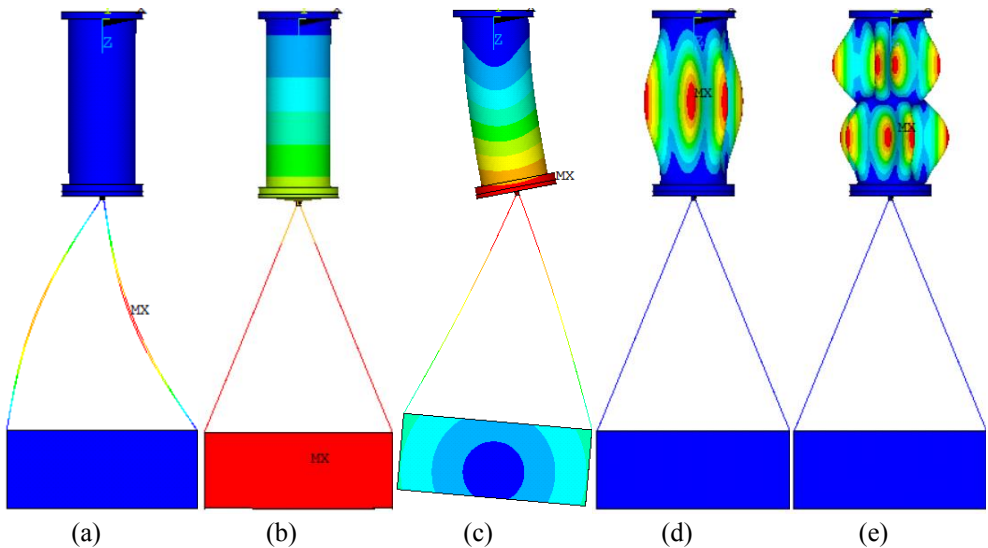


**Fig. 7.** Axial eigenmodes: (a) vibration mode in the wire rope; (b) mode (1,0); (c) mode (1,1); (d) mode (1,4); (e) mode (2,5) of the composite cylinder.

## 4 Conclusion

In current work, the FEM models of the composite cylindrical structure with and without the suspended weight were developed. For the models, natural frequencies and modes of vibrations were determined using the ANSYS Mechanical software package. An analysis of the influence of the suspended weight on the natural frequencies of vibrations is carried out. From the results obtained, the following conclusions can be drawn.

Static loads have an effect on the excitation frequency. For the model without basket with a weight, the increase of the value of the tensile force leads to increase of the vibration frequency, which is consistent with the known solutions available in the scientific literature. At that, the effect of load on the frequencies is not significant. The difference in natural frequencies of vibrations for the minimum and maximum values of tensile force does not exceed ~2%.

Composite cylinder with the suspended basket with the weight operates as a common system for the vibration modes (1,1) and (1,0), which leads to a decreasing the values of natural frequencies with an increasing the tensile force. For other modes of vibrations of the composite structure with the loaded basket, the values of natural frequencies coincide with the results of the modal analysis of the cylindrical composite structure with tensile force applied to the bottom end of cylinder or through the ring lug and do not exceed the percentage change of ~2%.

## Acknowledgments

This research was funded by the European Regional Development Fund Project No. 1.1.1.1/20/A/016 “A prototype of typical structural health monitoring system of operating objects for condition-based maintenance.”

## References

1. B. Wang, S. Zhong, T. L. Lee, K.S. Fancey, J. Mi, “Non-destructive testing and evaluation of composite materials/structures: A state-of-the-art review”, *Adv. Mech. Eng.* **12(4)** 1-28 (2020). DOI: 10.1177/1687814020913761
2. R. Kumpati; W. Skarka; S.K. Ontipuli, “Current Trends in Integration of Nondestructive Testing Methods for Engineered Materials Testing”, *Sensors* **21**, 1-32 (2021). DOI: 10.3390/s21186175
3. A. Kovalovs, M. Wesolowski, E. Barkanov and S. Gluhihs, “Application of Macro-Fibre Composite (MFC) as Piezoelectric Actuator”, *J. Vibroengineering* **11(1)**, 105-112 (2009).
4. E. Barkanov, M. Wesolowski, W. Hufenbach and M. Dannemann, “An Effectiveness Improvement of the Inverse Technique Based on Vibration Tests”, *Comput. Struct.* **146**, 152-162 (2015). DOI: 10.1016/j.compstruc.2014.10.006
5. E. Barkanov, A. Kovalovs, A. Anoshkin and P. Pisarev, “An Application of Thermal Analogy in Active Control Problems” In *Advanced Materials Modelling for Mechanical, Medical and Biological Applications. Advanced Structured Materials*, **155**. edited by H. Altenbach *et al.* (Springer International Publishing, Cham, Switzerland, 2022), pp. 152-162. DOI: 10.1007/978-3-030-81705-3\_4
6. E. N. Barkanov, “Method of Complex Eigenvalues for Studying the Damping Properties of Sandwich Type Structures”, *Mech. Compos. Mater.* **29(1)**, 90-94 (1993). DOI: 10.1007/BF00656275

7. E. Barkanov and J. Gassan, “Frequency Response Analysis of Laminated Composite Beams”, *Mech. Compos. Mater.* **30(5)**, 484 – 492 (1995). DOI: 10.1007/BF00616777
8. E. Barkanov, R. Rikards, C. Holste and O. Täger, “Transient Response of Sandwich Viscoelastic Beams, Plates and Shells under Impulse Loading”, *Mech. Compos. Mater.* **36(3)**, 215 – 222 (2000). DOI: 10.1007/BF02681873
9. M.P. Limongelli, E. Manoach, S. Quqa, P.F. Giordano, B. Bhowmik, V. Pakrashi, “Vibration Response-Based Damage Detection. In Structural Health Monitoring Damage Detection Systems for Aerospace”, edited by M.G.R. et al. (Springer International Publishing, Cham, Switzerland, 2021), pp. 133-174. DOI: 10.1007/978-3-030-72192-3\_6
10. F. Wei, Q. Pizhong, “Vibration-based Damage Identification Methods: A Review and Comparative Study”, *Struct. Health Monit.* **10(1)**, 83-111 (2010). DOI: 10.1177/1475921710365419
11. R. N. Arnold, & G. B. Warburton, “Flexural Vibrations of the Walls of Thin Cylindrical Shells Having Freely Supported Ends”, *Proc. Math. Phys. Eng. Sci. P ROY SOC A-MATH PHY*, **197(1049)**, 238–256 (1949). DOI: 10.1098/rspa.1949.0061
12. V.I. Weingarten, “Free vibrations of multilayered cylindrical shells”, *Exp. Mech.* **4**, 200–205 (1964). DOI: 10.1007/BF02323651
13. M. Amabili, “Nonlinear vibrations of laminated circular cylindrical shells: Comparison of different shell theories”, *Compos. Struct.* **94(1)**, 207–220 (2011). DOI: 10.1016/j.compstruct.2011.07.001
14. Y. Dong, H. Hu, L. Wang, “Critical examination on in-plane inertias for vibration characteristics of cylindrical shells”, *J. Sound Vib.* **511** 1-16 (2021). DOI: 10.1016/j.jsv.2021.116350
15. Den Hartog J.P. *Mechanical Vibrations* (Dover Publications, 1985).
16. W. Leissa, *Vibration of Shells* (NASA SP-288, US Government Printing Office, Washington DC, 1973)
17. W. Soedel, *Vibration of Shells and Plates* 2nded., (Marcel Dekker, New York, 1994)
18. J.B. Greenberg, and Y. Stavsky, “Vibrations and buckling of composite orthotropic cylindrical shells with nonuniform axial loads”, *Compos. B Eng.* **29(6)**, 695-70, (1998).
19. A. Yadav, M. Amabili, S.K. Panda, T. Dey, R. Kumar, “A semi-analytical approach for instability analysis of composite cylindrical shells subjected to harmonic axial loading”, *Compos. Struct.* **296**, 1-14 (2022). DOI: 10.1016/S1359-8368(98)00029-8
20. L. Tong. “Free Vibration of Axially Loaded Laminated Conical Shells”, *J. Appl. Mech.* **66(3)**, 758-763 (1999). DOI: 10.1115/1.2791722
21. R. Bedri & M. O. Al-Nais “Prestressed Modal Analysis Using Finite Element Package ANSYS International Conference on Numerical Analysis and Its Applications,” in Proceedings of the International Conference on Numerical Analysis and Its Applications, NAA:2004. June 29 - July 3, 2004, Rousse, Bulgaria, pp 171-178. DOI: 10.1007/978-3-540-31852-1\_19
22. G.R. Liu, S.S. Quek. *The Finite Element Method: A Practical Course*, 1st ed. (Butterworth-Heinemann: London, UK, 2003) pp. 180–184. DOI: 10.1016/C2012-0-00779-X
23. EN 338:2009. Structural timber. Strength classes. European Committee for Standardization (CEN), Brussels, 2009
24. <https://dynamica-ropes.com/dyneema-ropes/>

25. S. Rucevskis, A. Kovalovs, A. Chate, “Optimal Sensor Placement in Composite Circular Cylindrical Shells for Structural Health Monitoring,” in *5th International Conference: Innovative Materials, Structures and Technologies (IMST 2022)*, Journal of Physics: Conference Series 2423, edited by S. Rucevskis (IOP Publishing Ltd, Bristol, United Kingdom, 2022), pp. 1–9. DOI: 10.1088/1742-6596/2423/1/012021
26. R. Rikards, A. Chate, “Identification of elastic properties of composites by method of planning of experiments”, *Compos. Struct.* **42(3)**, 257 – 263 (1998). DOI: 10.1016/S0263-8223(98)00071-3
27. E. N. Barkanov, M. Wesolowski, P. Akishin and M. Mihovski (2018): “Techniques for Non-Destructive Material Properties Characterisation”, in *Non-Destructive Testing and Repair of Pipelines*, edited by E. N. Barkanov *et al.* (Springer International Publishing, Cham, Switzerland, 2018), pp. 191-207. DOI: 10.1007/978-3-319-56579-8\_13
28. A. Kovalovs, S. Rucevskis, “Identification of elastic properties of stiffened composite shell”, *Aviation.* **13(4)**, 101-108 (2009). DOI: 10.3846/1648-7788.2009.13.101-108
29. A. Mironov, A. Safonovs, D. Mironovs, P. Doronkin, V. Kuzmickis, “Health Monitoring of Serial Structures Applying Piezoelectric Film Sensors and Modal Passport”, *Sensors*, **23**, 1114 (2023). DOI: 10.3390/s23031114
30. R. Rikards, A. Chate, “Optimal design of sandwich and laminated composite plates based on the planning of experiments”, *Struct. Multidiscipl. Optim.* **10(1)**, 46 – 53 (1995). DOI: 10.1007/BF01743694
31. R. Rikards, A. K. Bledzkij, V. Eglajs, A. Chate, K. Kurek, “Elaboration of optimal design models for composite materials from data of experiments”, *Mech. Compos. Mater.* **28(4)**, 295–304 (1993). DOI: 10.1007/BF00616154